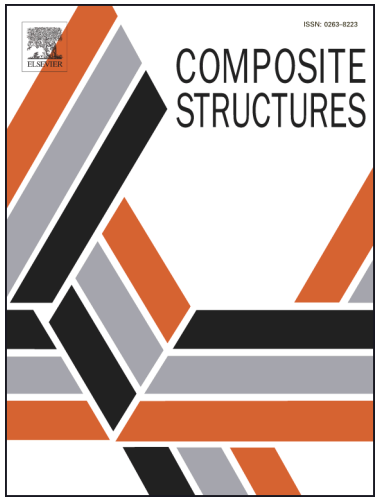

Design of the corrugated-core sandwich panel with external active cooling system

S.A. Lurie, Yu.O. Solyaev, A.A. Koshurina, V.F. Formalev, V.D. Dobryanskiy, M.L. Kachanov

PII: S0263-8223(17)33210-5
DOI: https://doi.org/10.1016/j.compstruct.2017.12.082
Reference: COST 9239

To appear in: *Composite Structures*

Received Date: 29 September 2017
Accepted Date: 28 December 2017

Please cite this article as: Lurie, S.A., Solyaev, Yu.O., Koshurina, A.A., Formalev, V.F., Dobryanskiy, V.D., Kachanov, M.L., Design of the corrugated-core sandwich panel with external active cooling system, *Composite Structures* (2017), doi: https://doi.org/10.1016/j.compstruct.2017.12.082

Design of the corrugated-core sandwich panel with external active cooling system

S.A.Lurie[a,b*], Yu.O.Solyaev[a,b], A.A.Koshurina[b], V.F. Formalev[c], V.D. Dobryanskiy[c], M.L. Kachanov[d,b]

[a]Institute of Applied Mechanics of Russian Academy of Science, Moscow, Russia
[b]Nyzhny Novgorod State Technical University named after R. E. Alekseev, Nyzhny Novgorod, Russia
[c]Moscow Aviation Institute, Moscow, Russia
[d]Department of Mechanical Engineering, Tufts University, Medford MA 02155, USA

Abstract

Optimal structure of thermal barrier skins used for rescue vehicles experiencing extreme conditions is developed. The conditions include extreme arctic cold and possible extreme heat of burning oil. The skin structure includes fibrous insulation material as well as external active cooling system using sprinklers. Optimal design variables, for the best combinations of the thermal and mechanical performances – the panel geometry and the discharge density – are examined by the analytic and numerical means. It is shown that the high discharge density in the cooling system may be necessary not only for the thermal protection, but also to provide the strength of the panel elements. In particular under the considered loading conditions, the solution of the optimization problem with all constraints exists only for the enough high discharge density due to the thermal buckling of the web elements inside the panel under non-uniform heating.

Keywords: sandwich panel, corrugated core, external active cooling, optimal structure

1. Introduction

We examine the optimal structure of thermal barrier skins used for the rescue vehicles experiencing extreme conditions. The conditions include extreme arctic cold and possible extreme heat (up to 1200 ^{o}C) of burning oil [1]. The skin structure includes fibrous insulation material as well as active cooling system using sprinklers. The optimal design, for the best combinations of the thermal and mechanical performances, involves the optimal choice of the panel geometry and of the discharge density.

Fiberglass is usually the structural material of choice for the similar vehicles or the freefall lifeboats; it possesses sufficient specific strength and stiffness. However, for the thermal protection against external cold and heat conditions the additional insulation is needed. As discussed in [1], [2], the use of only the passive thermal protection leads to substantial increase of panel thickness and weight that may be unacceptable. Hence the passive protection should be supplemented by an active external cooling (sprinkler system). The coolant in this system may be a seawater; however, in its absence, one may be compelled to use the onboard supply. This is the reason we consider not only the mass minimization problem, but, also, the minimization of the discharge density in the cooling system.

We consider a panel with a corrugated core. General principles of optimal design of such panels have been developed earlier (see, for example, [3], [4], [5], [6] and [7]). Note that sandwich panels with honeycomb core have higher mass efficiency, but their thermal protection characteristics are somewhat lower than those of corrugated core sandwiches, due to higher values of the effective thermal conductivity in the transverse direction [8], [9]. As far as foam

*Corresponding author. Email: salurie@mail.ru

core is concerned, it has good thermal insulation properties but poor mechanical characteristics [8], [9] and [10].

Sandwich panels with corrugated cores are often the best option for multifunctional structures: they have sufficient load bearing capacity and thermal protection [9]. The design of such panels has been discussed in a number of works; for the passive thermal protection, see the works [11], [12], [13] and [14]. It has been shown, in particular, that the conditions of thermal protection and thermal buckling of the core elements constitute the most serious constraint. It has also been found that analytical one-dimensional solutions allow one to obtain sufficiently accurate estimates of the thermal state of the panels under transient heating conditions across thickness. The panels with an internal active convective cooling system that use water were analyzed, in the context of structural an hydrodynamic parameters, in [14], [15], [16] and [17].

The present work aims at the optimization of geometry of a load-bearing and thermal protection panel with an active external cooling system. The interior of the panel contains an insulating fibrous material, to provide the passive thermal protection. We note that the active cooling system may be of three distinctly different types: transpiration, film cooling, and convective cooling [18]. The sprinkler system produces a "film" cooling (a thin layer of water flow on the vehicle surface). We proposed a simplified evaluation of the thermal state of the panel with such cooling system.

We solve the optimization problem using the methodology of optimization under constraints. Finite element simulations are carried out, and compared to the analytical solution. Optimal variants of panel structure are identified.

2. Modeling of the structure of the panel

We suggest simple analytical models for the effective thermal properties of the panel, for the cooling process, for the structural strength of the panel under mechanical loading and for thermal buckling of its elements caused by non-uniform temperature distribution.

2.1. Structure of the panel and its effective thermal properties

We consider a sandwich panel with corrugated core (a "web") shown in Figure 1 where notations are as follows. The face thickness is t_f, the web thickness is t_c and the core depth is h_c, The distance between the web elements is d_f, the corrugation pitch is $2p$, and the angle between the web and the vertical direction is θ. The total panel thickness is $h = h_c + 2t_f$. Total area of the load bearing elements in the panel cross section is $A = 4t_f p + 2t_c\left(d_f + h_c / \cos\theta\right)$. The panel length a = 1200 mm and its width b = 500 mm. Heat-insulating fibrous material fills the free space inside the panel. In the following, we use parameter $N = a / (2p)$ for the number of core pitches. Internal panel surface is located at $z = 0$ and the external one at $z = h$ in the coordinate system shown in Figure 1(b). The panel is placed on the lateral vertical wall of the vehicle that has mass M , length L, width is W, and height H.

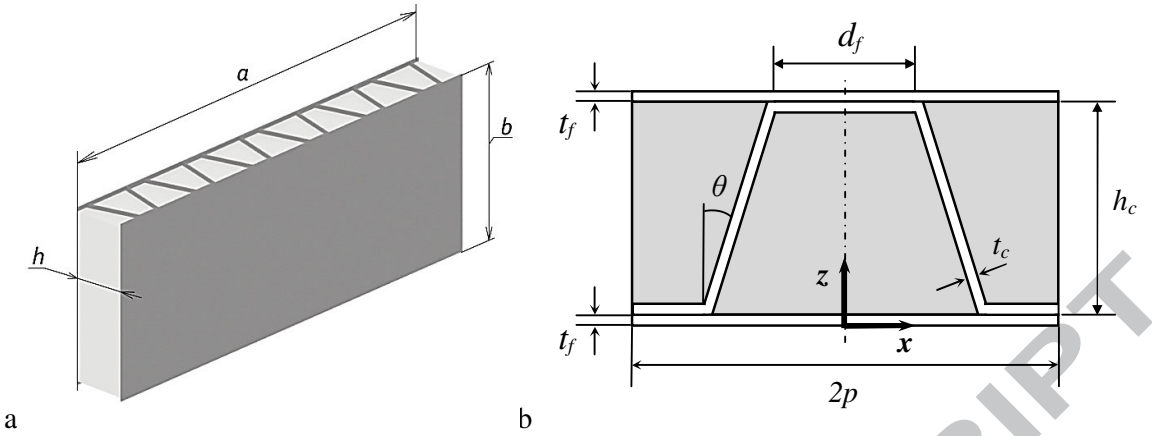

Fig. 1. Corrugated core sandwich panel (a) and its unit cell (b).

Thus, the average mass density of the panel is

$$\rho = \frac{2\rho_f V_f + \rho_c V_c + \rho_i V_i}{V} \tag{1}$$

The effective heat capacity and thermal conductivity, evaluated by the law of mixtures (that was shown in works [1, 11, 12] to be sufficiently accurate for the structures of this kind) are given by

$$c = \frac{2\rho_f c_f V_f + \rho_c c_c V_c + \rho_i c_i V_i}{\rho V} \tag{2}$$

$$k = \frac{2k_f V_f + k_c V_c + k_i V_i}{V} \tag{3}$$

where $V = 2ph$, $V_f = 2pt_f$, $V_c = 2t_c\left(d_f + h_c/\cos\theta\right)$, $V_i = V - 2V_f - V_c$.

2.2. Analysis of the external cooling process

For thermal protection of the vehicle, as it passes through burning oil, an external sprinkler system is used (Fig. 2). This system supplies water (or other cooling liquid) through the sprinkler heads mounted at the top of the vehicle; its temperature will be assumed T_0 = 20 °C. Water flows down along the outer surface of the vehicle under the action of gravity, thus protecting the vehicle. The discharge density η (that specifies how much water is spread, per minute, over a part of the cooled surface area of one square meter) is usually below 20 *liter·min*$^{-1}$·*m*$^{-2}$ (or 3.33 10^{-4} *m/s* in the Si-system).

For the analysis of the cooling process, the following assumptions will be used:

1) The flow of water is laminar, of constant thickness h_w (Fig. 2);
2) The flow is uniformly heated through the thickness to temperature $T_w(t, y)$;
3) No boiling occurs;
4) The heat dissipation due to evaporation is neglected.

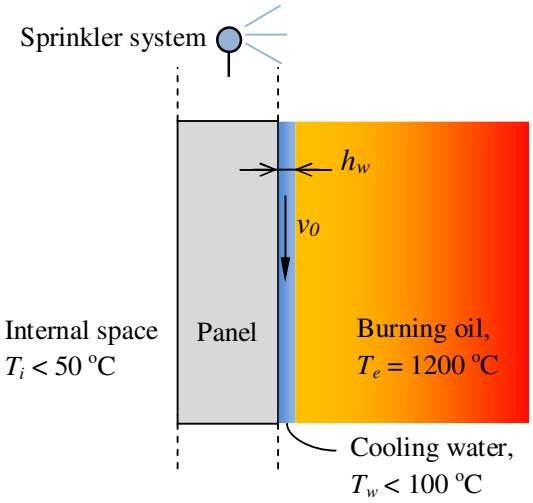

Fig. 2. Model of the external active cooling system

The thickness of the water flow h_w is controlled by the discharge density η and flow velocity v_w. Water moves, driven by gravity, along the vertical wall of the vehicle having height H. The flow velocity at the lower edge of the vehicle body ($y = H$) is $v_w = \sqrt{2gH}$. The discharge density η is the ratio of the water volume flowing, per second, over a part of the vehicle surface of the area of 1 m^2. Then,

$$\eta = \frac{v_w h_w}{H} \quad \text{so that} \quad h_w = \eta\sqrt{\frac{H}{2g}} \tag{4}$$

To estimate the maximal temperature $T_{w,\max}$ to which the water is heated during its run along the vehicle surface. We assume Newton's law for the heat transfer between layer of cooling water and external environment and a thermal insulation condition between water and vehicle's body. Neglecting the conductive heat transfer in the direction of flow, one obtains the following relation for a unit volume of the cooling water:

$$\alpha_w\left(T_e - T_w\right) = c_w\rho_w h_w \frac{\partial T_w}{\partial t} \tag{5}$$

where α_w is the coefficient of heat transfer across the boundary between the flow and the external environment, T_e is the (elevated) temperature of the external environment, and c_w, ρ_w are the heat capacity of the water and its density.

Solving equation (5) with the initial condition $T_w = T_0$ and taking into account that the time the water spends on the vehicle's surface is $\sqrt{H/2g}$, and also taking into account (4), we find the maximal temperature of water:

$$T_{w,\max} = T_e - \left(T_e - T_0\right)e^{-\frac{\alpha_w}{c_w\rho_w\eta}} \tag{6}$$

We now obtain the upper and lower bounds of the discharge density that ensures the required thermal protection of the structure. To obtain the lower bound, it is assumed that the maximal temperature of the water $T_{w,\max}$ should not exceed its boiling point T_b. Then equation (6) implies that

$$\eta_{\min} = \frac{\alpha_w}{c_w \rho_w \ln\left((T_e - T_0)/(T_e - T_b)\right)} \tag{7}$$

The upper bound η_{upp} follows from the condition that the temperature of the water, and therefore the temperature of the outer surface of the panel, should not exceed a given permissible value $T_{\max}$ that is determined by the safety conditions (see Section 2.3 below). Then

$$\eta_{\max} = \frac{\alpha_w}{c_w \rho_w \ln\left((T_e - T_0)/(T_e - T_{\max})\right)} \tag{8}$$

2.3. Thermal analysis

The two basic insulating functions of the panel are: thermal insulation under cold environment conditions and thermal protection under intense heating (burning oil). In the first case, the temperature of the inner surface of the panel T_{wi} should be above the prescribed temperature $T_{\min}$ (safety requirement). The value T_{wi} is determined from the solution of the steady-state heat conduction problem. Thus, we obtain the first optimization constraint (as discussed in detail in [1]):

$$T_{wi} = T_i + \frac{(T_e - T_i)/a_i}{h/k + 1/a_e + 1/a_i} \geq T_{\min} \tag{9}$$

where T_e, T_i are air temperatures outside and inside the vehicle and a_e, a_i are the heat transfer coefficients on the external and inner surfaces of the panel.

In the second constraint (motion in the burning oil field for the specified time period Δt) the external cooling system operates. Eq. (6) determines the maximal temperature of the coolant flowing along the panel surface – which is also the temperature on the external panel wall. To determine the temperature distribution in the panel, we need to solve the transient heat conduction problem with the condition that constant temperature $T_{w,\max}$ given by (6) is prescribed on its outer surface for a period of time Δt. On the inner surface, we assume the thermal insulation condition. Thus, we consider the following problem:

$$\begin{aligned} &0 < z < h: \quad c\rho \frac{\partial T}{\partial t} = k \frac{\partial^2 T}{\partial z^2}, \\ &z = 0: \ \frac{\partial T}{\partial x} = 0, \quad z = h: \ T = T_{w,\max}, \quad t = 0: \ T = T_0. \end{aligned} \tag{10}$$

The solution of this problem can be found analytically [19]. The solution of the problem (10) yields the second constraint: the maximal temperature of the inner surface of the panel $z = 0$ that is realized after time period Δt should not exceed a given permissible value $T_{\max}$:

$$T_{wi,\max} = T_{w,\max} - 2\left(T_{w,\max} - T_0\right) \sum_{n=0}^{\infty} \frac{(-1)^n}{p_n} e^{-p_n^2 W \Delta t} < T_{\max} \tag{11}$$

where $p_n = (2n+1)\pi/2$, $W = k/\left(c\rho h^2\right)$.

Note that all the assumptions made in derivation of condition (11) provide us a reserve for the heat protection parameters. We neglected the initial velocity of the coolant to determine the flow velocity, neglected its evaporation, used the maximum temperature of coolant to assess the thermal state of the panel, and we assumed the thermal insulation conditions in solving problems (5) and (10).

2.4. Strength analysis

We discuss requirements on strength of the panel under different loading conditions – both static and dynamic – that correspond to different working regimes of the vehicle. Restrictions for the strength, stability and thermal stability of panel elements are specified.

2.4.1. Compression

The maximal compression resultant force N_y (in the parallel to the panel direction y) corresponds to the case when the vehicle overturns and lands on its roof. Assuming, for simplicity, the uniform normal traction boundary conditions we have the same normal stress $\sigma_y = 2pN_y/A$ in both face sheets and the core. If the boundary load – and hence the stress – are sufficiently high, one of the three possible failure mechanisms can be identified: fracture of the bulk material, as induced by the compressive stress; buckling of the face sheet, and buckling of web elements. Using known results [4, 20] for the critical stress that causes buckling, we have the following critical conditions corresponding to the mentioned mechanisms:

$$\begin{aligned} &\sigma_y = \sigma_{ult} && \text{face or web failure} \\ &\sigma_y = \frac{\pi^2 E t_f^2}{3\left(1-\nu^2\right)\left(2p-d_f\right)^2} && \text{face sheet buckling} \\ &\sigma_y = \frac{\pi^2 E t_c^2 \cos^2\theta}{3\left(1-\nu^2\right)h_c^2} && \text{web element buckling} \end{aligned} \qquad (12)$$

where σ_{ult} is compressive strength of the panel material.

2.4.2. Shear

In the case of asymmetric motion over an obstacle, the vehicle body is twisted and resultant shear force N_{xy} occurs in the panel. This force is primarily resisted by the panel faces. Shear stress in the faces is $\tau_{xy} = N_{xy}/(2t_f)$. The critical stresses under shear are [4, 20]:

$$\begin{aligned} &\tau_{xy} = \tau_{ult} && \text{face or web failure} \\ &\tau_{xy} = \frac{\pi^2\sqrt{2}E t_f^2}{3\left(1-\nu^2\right)\left(2p-d_f\right)^2} && \text{face sheet buckling} \\ &\tau_{xy} = \frac{\pi^2\sqrt{2}E t_c^2 \cos^2\theta}{3\sin\theta\left(1-\nu^2\right)h_c^2} && \text{web element buckling} \end{aligned} \qquad (13)$$

where τ_{ult} is shear strength of the panel material.

2.4.3. Impact

In a preliminary design, we assume that, under impact with flat obstacle, the uniform pressure q acts on the lateral surface of the vehicle with area $L \times H$. The compression of the panel in the transverse direction is primarily resisted by the web elements. The mean relative displacement between the outer and the inner faces of the panel is δ. This displacement determines the work of external forces done under impact. For the given initial vehicle velocity v_0, pressure q can be estimated from the energy consideration as $q = Mv_0^2/(2\delta LH)$. Displacement δ can be

evaluated as $\delta = \varepsilon_{\max} h_c \cos\theta$ if the maximum strain in the web elements $\varepsilon_{\max}$ is known. Thus, we find the value of pressure:

$$q = \frac{M v_0^{\,2}}{2\delta LH} = \frac{M v_0^{\,2}}{2\varepsilon_{\max} h_c LH \cos\theta} \tag{14}$$

Compression normal stress in the web elements σ_w can be estimated from the equilibrium equation in the *z* direction:

$$\sigma_w = \frac{pq}{t_c \cos\theta} \tag{15}$$

The critical normal stress for the web element under compression is [21]:

$$\sigma_{cr} \cong \frac{2\pi^2 E}{\left(1-\nu^2\right)}\left(\frac{t_c \cos\theta}{h_c}\right)^2 \tag{16}$$

Using equations (14)-(16) and assuming that maximum strain in the web elements under impact loading is proportional to its critical buckling strain under static loading i.e. $\varepsilon_{\max} = n\varepsilon_{cr} = n\sigma_{cr}\left(1-\nu^2\right)/E$, we could derive the condition of web element stability under impact in the form:

$$\frac{8n\pi^4 E t_c^{\,5} \cos^6\theta}{\left(1-\nu^2\right) h_c^{\,3} p} > \frac{M v_0^{\,2}}{LH} \tag{17}$$

The coefficient *n* can be determined based on comparison of (17) with FE transient structural analysis with large deflection effects. As it will be shown below, the optimal value of this coefficient is $n = 32$.

2.4.4. Thermal buckling

Due to non-uniform heating of the panel, thermal buckling of web elements inside it may occur, reducing the load-bearing capacity of the panel. To prevent such effects, we introduce an additional thermal buckling condition in the thermo-structural optimization problem based on the known analytical solution [22]. In this solution, a rectangular simply-supported plate is considered. Long edges of the plate can move freely in the normal in-plane direction, and the short edges are fixed in the normal direction. Temperature variation is realized along the short edges. Using this model for the web elements which short edges height is $h_c / \cos\theta$, we find that thermal buckling occurs if their average temperature $\overline{T}$ reaches a critical value [22]:

$$T_{cr} = T_0 + \frac{\pi^2 t_c^2 \cos^2\theta}{3(1-\nu^2) h_c^2 \alpha} \tag{18}$$

where T_0 is the initial temperature of the panel provided there are no thermal stresses and α is the coefficient of thermal expansion.

Note that condition (18) includes an average temperature of the web elements only; it does not take into account the temperature distribution. The use of such estimate is possible if the temperature gradients are not overly large as is the case in the considered problem. We also note that the condition (18) assumes that the thickness of the panel can freely increase due to heating, but its in-plane displacements are equals zero, due to the fact that the panel is placed on a rigid frame, which is heated up more slowly.

2.5. Optimization

The goal is to find the geometric parameters t_f, t_c h_c.d_f, and N that minimize the mass per unit area of the panel. We also need to determine the discharge density required in the external cooling system: it should be as small as possible, as the amount of available water may be limited. Mass per unit area of the panel is calculated, taking into account (1) as $m = \rho h$.

The value of discharge η is determined from (11) taking into account (6), or directly using bounds (7), (8) in which the discharge is determined only through the given physical properties of water and the parameters of heat exchange with the external environment.

The constraints in the optimization problem are formulated using safety factors. Based on (9), (11), (12), (13), (17) and (18) we introduce the following safety factors:

$$K_{T,\min} = T_i + \frac{(T_e - T_i)/a_i}{h/k + 1/a_e + 1/a_i} - T_{\min}$$ insulation under cooling

$$K_{T,\max} = T_{\max} - \left(T_{w,\max} - 2(T_{w,\max} - T_0) \sum_{n=0}^{\infty} \frac{(-1)^n}{p_n} e^{-p_n^2 W \Delta t} \right)$$ protection under heating

$$K_y = \frac{\sigma_{ult}}{\sigma_y}$$ failure under compression

$$K_{y,f} = \frac{\pi^2 E t_f^2}{3\sigma_y (1-\nu^2)(2p - d_f)^2}$$ face buckling under compression

$$K_{y,c} = \frac{\pi^2 E t_c^2 \cos^2\theta}{3(1-\nu^2) h_c^2 \sigma_y}$$ web buckling under compression

$$K_{xy} = \frac{\tau_{ult}}{\tau_{xy}}$$ failure under shear

$$K_{xy,f} = \frac{\pi^2 \sqrt{2} E t_f^2}{3\tau_{xy} (1-\nu^2)(2p - d_f)^2}$$ face buckling under shear

$$K_{xy,c} = \frac{\pi^2 \sqrt{2} E t_c^2 \cos^2\theta}{3\sin\theta (1-\nu^2) h_c^2 \tau_{xy}}$$ web buckling under shear

$$K_z = \frac{64\pi^4 E t_c^5 \cos^6\theta LH}{(1-\nu^2) h_c^3 p M v_0^2}$$ web buckling under impact

$$K_{T,buckl} = \frac{\pi^2 t_c^2 \cos^2\theta}{3(1-\nu^2) h_c^2 \alpha (\overline{T} - T_0)}$$ web thermal buckling

where $\sigma_y = 2pN_y / A$, $\tau_{xy} = N_{xy} / (2t_f)$ are the stresses, which are determined by a given loading level, v_0 is an initial speed of the vehicle in the impact problem, $\overline{T}$ is an average temperature of the web elements in the intense heating problem.

Solution of the optimization problem is found using Wolfram Mathematica system using special numerical nonlinear global optimization method called “simulated annealing”, with predefined ranges of geometric parameters. If we determined that some parameters of the optimization problem are not essential and could be set to its minimum or maximum values in

the predefined ranges, then the solution is iterated one more time with fixed values of these parameters. Such iterations allows one to refine the solutions.

To verify the optimal design calculations, we conduct the FE modeling using the Ansys package. The temperature problems will be solved in a 2-D formulation. Strength analysis is carried out on a 3D geometry of the panel's unit cell, built with the Mindlin-Reussner plate elements. The influence of the heat-insulating fibrous material on the mechanical behavior of the structure is neglected.

3. Results and discussion

In the preliminary design, we consider the prismatic form of the vehicle body with length L = 8.5 m, width W = 3.3 m and height H = 2.2 m, the total mass is M = 13 t. These parameters satisfy the usual requirements for these vehicles. Material of the panel faces and core is glass fiber reinforced plastic (GFRP). All laminates assumed to be quasi-isotropic and symmetric In the internal free space of the panel, a rockwool fibrous thermal insulation material is placed. Water is used in the external cooling system. Material properties used in the estimations are presented in Table 1. The ranges of design variables are presented in Table 2; that take into account technological limitations.

Table 1. Materials properties

Material	ρ kg/m^3	k W m^{-1}C^{-1}	c J kg^{-1}C^{-1}	α 10^{-6}C^{-1}	E GPa	v	σ_{ult} MPa	τ_{ult} MPa
GFRP	1800	1	1000	25	22	0.25	380	45
Rockwool	25	0.03	1000	-	-	-	-	-
Water	1000	0.6	4200	-	-	-	-	-

Table 2. Ranges of the design variables

Parameter		Minimum value	Maximum value
t_c	mm	0.5	2
t_f	mm	1	4
h_c	mm	20	200
d_f	mm	0	p^*
N	-	10	20

*Web core is triangular if $d_f = 0$ and rectangular if $d_f = p = a/(2N)$

The main conditions for the temperature and mechanical loading of the panel have been formulated in the earlier work [1], [2]. The minimal temperature of the external environment in formula (9) should be taken as $T_e = -50\,^oC$; the temperature inside the vehicle is $T_i = 20\,^oC$. The minimal allowable temperature of the panel inner surface is $T_{\min} = 12\,^oC$. The heat transfer coefficients in (9) are assumed to be $a_i = 5$ W m^{-2} K^{-1} (free convection) and $a_e = 20$ W m^{-2} K^{-1} (forced convection under conditions of strong wind and high humidity).

The maximal allowable time of the vehicle moving in the burning oil field (the outside temperature $T_e = 1200\,^oC$) is Δt = 8 min. The coolant temperature is $T_0 = 20\,^oC$, and the

maximal allowable temperature of the inner surface of the panel is $T_{\max} = 50\,^{o}C$. The theory of heat transfer [23] implies then that the heat transfer coefficient between the cooling water flow and external environment at given elevated temperature should be about $\alpha_w = 20$ W m^{-2} C^{-1}.

On the basis of (7) and (8), we obtain the upper and lower bounds of the discharge density in the cooling system. Given that the coolant is water, which should not overheat above $T_{\mathrm{w,max}} = 90\,^{o}C$, we find the lower bound $\eta_{\min}$ = 4.7 liter·min^{-1}·m^{-2}. The upper bound follows from the condition that $T_{\mathrm{w,max}} = T_{\max} = 50\,^{o}C$, and therefore $\eta_{\max}$ = 11.1 liter·min^{-1}·m^{-2}.

The maximal compression force per unit of the panel length that occurs due to overturning of the vehicle can be estimated as: $N_y = M\,g\,/\left(2\left(L+W\right)\right) \approx 5400$ N/m. The maximal torque in the vehicle caused by asymmetric driving over an obstacle is $M_t \approx$ 8800 N·m (as determined by FE calculations for similar metal structures, from the typical condition that their maximal twisting angle is 3^{o}). The shear force per unit of the panel length determined from the solution of the strength of materials problem for the thin-walled section (vehicle body) torsion is: $N_{xy} = M_t\,/\left(2HW\right) \approx$ 600 N/m. To estimate the load during impact, the initial vehicle speed, at the moment of impact, is assumed to be 2 m/sec.

3.2. Optimal thermal performance

At first, we find the geometry of the panels that ensures optimal thermal performance under cooling and heating conditions. We consider two limiting cases, for the minimal and maximal water discharge density (7), (8), that is necessary under conditions of intense heating. Thus, the optimal panel configuration corresponding to minimum mass is found from solution of the following problem:

$$\begin{cases} m(t_f, t_c, h_c, d_f, N) \to \min, \\ \eta = \eta_{\min} \;\; or \;\; \eta = \eta_{\max} \;\;,\;\; K_{T,\min} > 0,\;\; K_{T,\max} > 0 \end{cases} \tag{19}$$

Solution of this problem is the geometry of the panel with minimal thickness of the load bearing elements and with triangular core with maximal angle of inclination allowable for the considered total width of the panel (see Fig. 3(a) and Table 3). The only essential parameter in the optimization problem (19) is core depth h_c, and the other design parameters could be set to its minimum values in the predefined ranges. The panel mass per unit area is 7.4 kg/m^2 and the total thickness is 91 mm.

In problem (19), the condition for thermal insulation at low temperatures $K_{T,\min} > 0$ is most important; it determines the value of core depth h_c. The good consistency of analytical and numerical predictions with respect to this condition has been demonstrated in the earlier work [1]. Condition at elevated temperature $K_{T,\max} > 0$ is satisfied in the problem (19) with a large margin, which means that it is sufficient to use the minimum water flow $\eta_{\min}$ in the cooling system in the calculations. However, it is important to check this result using FE calculations. This is necessary, since the analytical solution does not take into account the fact that after leaving of the vehicle from a burning oil field, the temperature of internal surface of the panel can continue to rise because of the spreading of heat accumulated inside its core [1].

In FE simulations, we assume that, on the outer surface of the panel during the above-mentioned 8 minutes period, temperature is $T_{w,\max} = 90\,^{o}C$. Then the structure cools down under

conditions of free convection, at ambient temperature of $T_0 = 20\,^oC$. On the outer surface of the panel in this case we set the heat transfer condition according to Newton's law, with the heat transfer coefficient 5 W m^{-2} K^{-1}. On the inner surface of the panel we use the thermal insulation condition. The results of the calculations are shown in Figure 4. It is shown here that the analytical solution uields a sufficient thickness of the panel for a given minimum discharge $\eta_{\min}$ that provides heat protection of the internal space of the structure. The temperature of the inner surface of the panel reaches an acceptable maximum $T_{wi,\max} \approx 23\,^oC$ half an hour after the end of the intense heating (Fig. 4(b)).

Table 3. Parameters and safety factors of panels that are optimized based on thermal, mechanical and thermomechanical analyses

Parameter		Optimal thermal performance	Optimal mechanical performance	Optimal thermomechanical performance
t_f	mm	1	1	1
t_c	mm	0.5	0.5	1.25
h_c	mm	89	20	108
d_f	mm	0	53	29
N	-	10	10	10
θ	deg	33.5	19.3	16.3
h	mm	91	22	110
m	kg m^{-2}	7.4	5.2	11.4
η	liter m^{-2} min^{-1}	4.7	-	10.5
$K_{T,\,min}$	deg	0	-	0
$K_{T,\,max}$	deg	29.9	-	29.9
K_y	-	-	22	41
$K_{y,f}$	-	-	1	1
$K_{y,c}$	-	-	2.5	1
K_{xy}	-	-	148	148
$K_{xy,f}$	-	-	80	43
$K_{xy,c}$	-	-	600	153
K_z	-	-	9.7	6.1
$K_{T,\,buckl}$	-	-	-	1.06

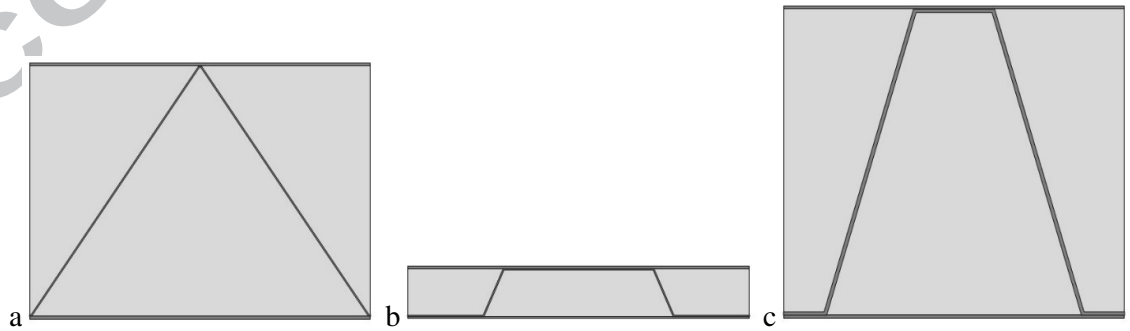

Fig. 3. Geometry of the unit cell with optimal thermal (a), mechanical (b) and thermomechanical (c) performance

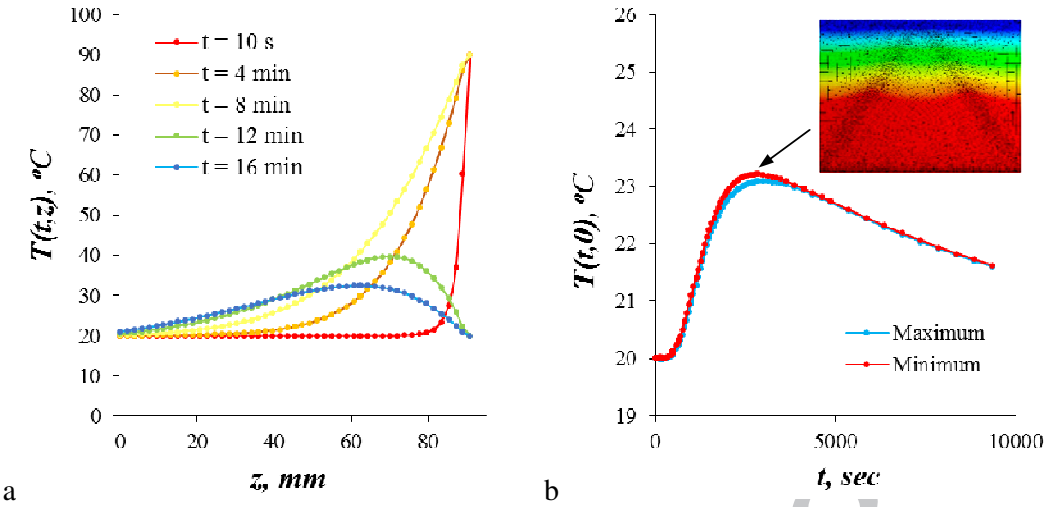

a b

Fig. 4. Results of FE modeling of the process of heating and subsequent cooling of panel for a minimum water discharge density $\eta_{\min}$ in the cooling system, (a) the distribution of panel temperature across the thickness at different time moments, (b) the variation of the maximal and minimal temperature of the inner surface of the panel with time; the temperature distribution in unit cell is shown at the time of maximum heating of the bottom surface.

3.2. Optimal mechanical performance

We consider the following optimal design problem: Find the geometry of the panel with minimal mass and satisfying structural strength constraints:

$$\begin{cases} m(t_f, t_c, h_c, d_f, N) \to \min, \\ K_y > 1,\ K_{y,f} > 1,\ K_{y,c} > 1,\ K_{xy} > 1,\ K_{xy,f} > 1,\ K_{xy,c} > 1,\ K_z > 1 \end{cases} \tag{20}$$

The solution of this problem implies that the panel with optimal mechanical properties has the smallest overall thickness of 22 mm and almost rectangular web (see Fig. 3b and Table 3). The most significant restriction in the search for the solution is the stability condition of face sheets under compression $K_{y,f} > 1$. It is seen from Table 3 that four other geometric parameters can be fixed in the search. Face and web thickness, core depth and number of corrugation pitches over the panel length could have minimum allowable values and only the distance between the web elements should be selected in such a way that the faces and web elements are rather narrow and do not lose stability.

The applied strength and stability conditions in problem (20) are quite common and have been well-tested [1, 3, 4, 5, 7, 21]. The condition of stability of web elements under impact (17) is non-trivial and requires numerical verification.

The FE simulation of the impact of the panel was done in the Ansys system, in the module for transient analysis using finite strain formulation. A fragment of the panel with optimal mechanical performance was considered; it had length of 100 mm and width of one core wave, that, in the case of an optimum geometry, is 120 mm (Fig. 5a). To be able to simulate the effect of buckling, web elements in the panel were built with given small curvature. The radius of their curvature is 10 m while its height is about 2 cm. Such geometry, with "almost straight web elements", allows modeling the effects of stability loss in nonlinear transient calculations. At edges of the panel, periodic boundary conditions were set. The initial velocity of the entire model was determined in the vertical direction. On the lower surface of the panel, the distributed mass

related to the given dimensions of the fragment was set. On the top surface of the panel, the condition of contact with a flat obstacle was used by setting zero vertical displacements. The problem was solved for the first 2 seconds of the impact, without damping.

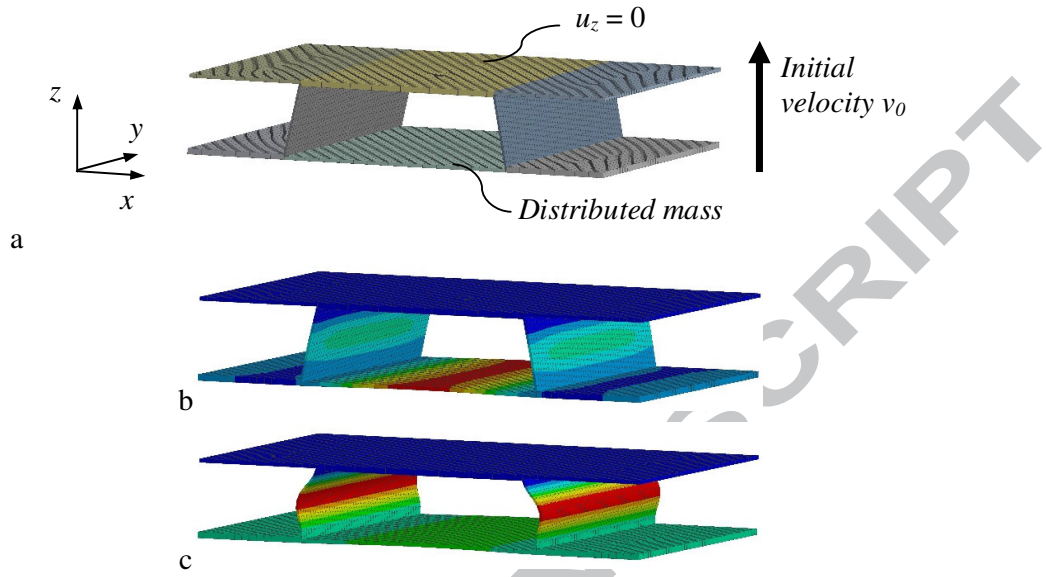

Fig. 5. Transient simulations of the panels fragment under impact,
a: loading scheme, b: stability of the web elements under low speed of the impact, c: buckling of the web elements under high speed of the impact. The color in figures *b* and *c* shows the magnitude of the total displacements. Real scale of deformations is used.

The calculations determine that the deformed state of the panel. It has been found that, at low impact velocities, the web walls retain their shape (Fig. 5b); however, if the impact velocity exceeds certain critical value $(v_0)_{cr}$, the deformation pattern of the walls changes – the buckling and bending are observed (Fig. 5c). Thus, the 3D model predicts buckling of web elements under impact. We also varied the thickness of web elements and determined the speeds $(v_0)_{cr}$ that lead to the web elements buckling.

The dependence of the critical impact velocity $(v_0)_{cr}$ on the thickness of web elements t_c is shown in Figure 6 where points show the results of numerical simulation, and lines show the analytical predictions obtained from condition (17). If in this condition we assume the equality, take $n = 32$, express v_0 in t_c, and take the values of all other parameters from the initial data and solution of the problem (20) (see Table 3), we obtain $v_0 \approx 7\sqrt{n\, t_c^{\,5}}$. This dependence is shown in Figure 6 by lines, for different values of n. It is seen that the analytical solution agrees well with numerical calculations for $n = 32$. In this case, the criterion used in the design $K_z > 1$ can be considered as reliable. We note that due to the presence of damping in the real construction, the critical impact velocities will be higher and in fact an additional strength margin will be realized.

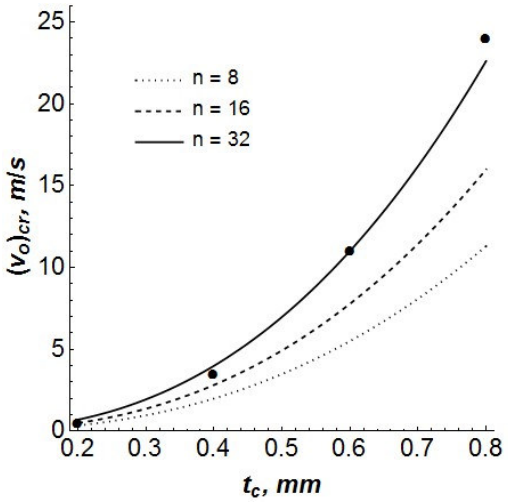

Fig. 6. Dependence of the impact critical velocity $(v_0)_{cr}$ that induced the web elements buckling on web thickness t_c. Analytical solution is shown by lines, FE simulation – by points.

3.3. Optimal combined thermo-structural design

We now consider the optimization problem taking into account all of the constrains for thermal protection and strength, and also taking into account the possibility of variation of the water discharge density in the external cooling system:

$$\begin{cases} m(t_f, t_c, h_c, d_f, N) \to \min, \\ \eta_{\min} \le \eta \le \eta_{\max}, \ K_{T,\min} > 0, \ K_{T,\max} > 0, \\ K_y > 1, \ K_{y,f} > 1, \ K_{y,c} > 1, \ K_{xy} > 1, \ K_{xy,f} > 1, \ K_{xy,c} > 1, \ K_z > 1, \ K_{T,buckl} > 1 \end{cases} \quad (21)$$

The solution of problem (21) is the geometry of the panel shown in Figure 3c. Parameters of the panel optimal geometry are presented in Table 3. The unit cell of the panel has sufficiently large total thickness to satisfy the requirements of thermal protection. Due to this, it is necessary to increase the web thickness, to prevent its buckling under mechanical loading and under non-uniform heating. This leads to an increase of the panel mass.

Essential constraints in problem (21) are the thermal insulation condition at low temperatures $K_{T,\min} > 0$, the condition of faces stability under compression $K_{y,f} > 1$ and conditions of web stability under compression $K_{y,c} > 1$ and under non-uniform heating $K_{T,buckl} > 1$. Note that the last condition can be satisfied only by lowering the temperature of the panel heating. Hence it is necessary to set an increased discharge density in the cooling system $\eta > \eta_{\min}$. The not essential parameters of the problem (21) are the faces thickness and the number of web pitches over panel length. The solution has monotone dependence on them, thus we assign them the minimum values in the predefined ranges (see Table 3).

Based on the obtained results shown in Figure 7, the failure/thermal protection map is constructed for the variation of core depth and web thickness and for different discharge densities in the cooling system. It is seen that, if the minimal discharge density is used, the problem (21) has no solution. In this case, the web thermal stability area of parameters values do not overlap with the areas of other criteria satisfaction (see red dotted line in Fig. 7). As the discharge in the cooling system increases, the panel temperature decreases and the web thermal buckling criterion shifts higher (black dashed line in Fig. 7). Thus, a region of optimal values can be identified (shaded area in Fig. 7). The minimum mass of the panel is realized for the

minimum allowable values of the parameters found from the solution of the optimization problem. This solution is shown by the point in Figure 7.

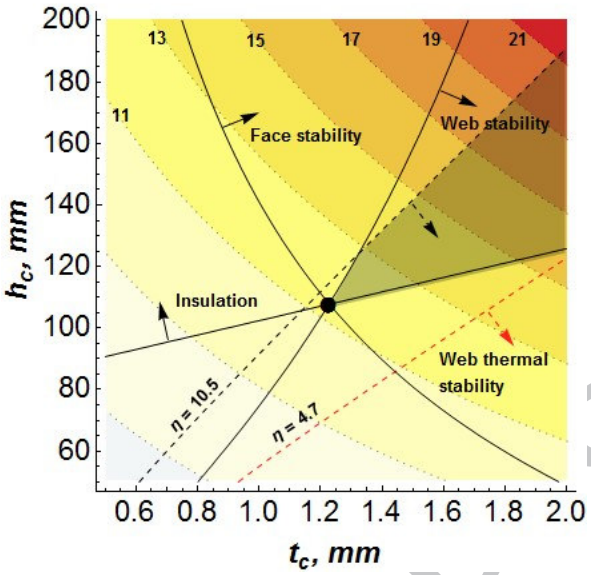

Fig. 7. Failure mechanisms/thermal protection map for the corrugated core sandwich panel optimized for the best thermo-structural performance, $t_f = 1$ mm, $d_f = 29$ mm, $N = 10$. The color and numbers indicate the mass of the panel unit area in kg/m^2. The shaded area presents the ranges of the parameters values that provide the satisfaction of all constraints. The point is the solution of optimization problem.

The found optimal variant of the geometry (Fig. 3c) must be verified in FE simulation. Of all the restrictions we used, the condition for the thermal buckling of the web elements has not been verified, which in this case turned out to be the most important one in the problem (21). To test it, we perform FE modeling of thermomechanical behavior of the panel under non-uniform heating. As shown in [11], the web thermal buckling in the corrugated core sandwich panel occurs at maximal temperature drop between its outer and inner surfaces. In the considered problem, the maximal temperature difference (~20/90°C) occurs during the first eight minutes of heating. The maximal average panel temperature is realized at the end of this period.

Thus, in the FE thermomechanical simulations we specify the temperature field realized in the panel after 8 minutes of heating. This temperature distribution, found from the 2-D heat conduction problem, was prescribed in the 3-D model (Fig. 8a). Buckling analysis was carried out based on the static thermoelasticity solution in the Ansys system. At the edges of the unit cell in the direction of corrugation, the periodic boundary conditions were set. It has been found that for the optimal panel geometry (Fig. 3c) the buckling safety factor is 2.34 and the first buckling mode refer specifically to the web elements (Fig. 8b).

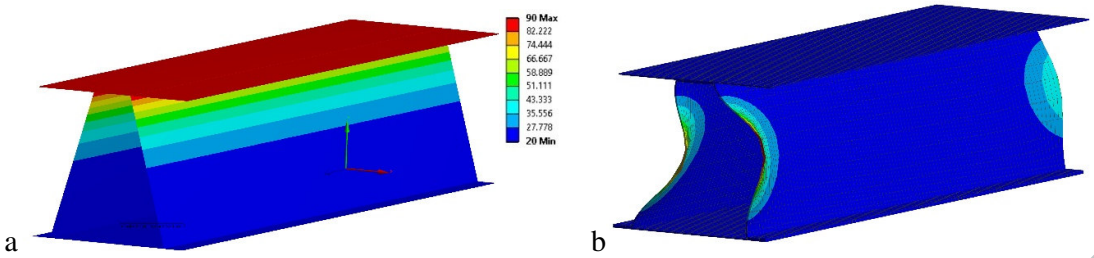

Fig. 8. a: Prescribed temperature distribution in FE simulations, b: the first buckling mode under non-uniform heating of the panel's unit cell.

4. Conclusions

Optimal design solutions for the corrugated core sandwich thermal barrier panel are presented. It is shown that thermal protection under the conditions of burning oil field can be provided using an active external cooling system. However, it is not enough to use the minimal discharge density in the cooling system, since, in addition to thermal protection, this system must ensure the preservation of the load bearing capacity of the structure. Using increased discharge ensures stability of the web elements under non-uniform heating inside the panel.

As found from the thermo-structural optimization, the panel geometry (Fig. 3c) is not the intermediate one, between the optimal variants found for the best mechanical or thermal performance separately (Figs. 3a, b). In the combined thermo-structural problem, it is necessary to increase the total thickness of the panel to meet the requirements of the thermal protection, which leads to increase the thickness of the web elements to prevent buckling under compression, impact or non-uniform heating of the panel. As web thickness increases, the equivalent thermal conductivity of the panel also increases, and this leads to the need for an additional increase of its total thickness. These iterations converge, but the optimal geometry of the panel has a greater total thickness and a larger mass, than the panels designed only with constrains of mechanical strength or heat protection.

To further improve the considered structure, it is necessary to solve the problem of stability of face and web elements under mechanical and thermal loads. These are the main criteria that limit the strength of the panel (see Table 3). Solution of this problem is possible, e.g. with the use of foam insulation instead of fibrous one inside the corrugated core of the panel. The foam insulation has relatively high stiffness, and it must prevent the stability loss of the panel elements, see [24], [25]. However, the thermal conductivity and density of the foams are higher than the thermal conductivity of fibrous materials, so the efficiency of the foam-filled corrugated core sandwich panels should also be checked in the context of the corresponding optimization problem.

Acknowledgements

This work was supported by the Russian Government under grant "Measures to Attract Leading Scientists to Russian Educational Institutions" (contract No. 14.Z50.31.0036).

References

1. Lurie, S. A., Solyaev, Y. O., Volkov-Bogorodskiy, D. B., Bouznik, V. M., & Koshurina, A. A. (2017). Design of the corrugated-core sandwich panel for the arctic rescue vehicle. Composite Structures, 160, 1007-1019.
2. Bouznik, V. M., Lurie, S. A., Solyaev, Y. O., Dudchenko, A. A., Volkov-Bogorodsky, D. B., Koshurina, A. A. (2016). Designing a multilayer panel with heat-insulating filler and

heat-shielding external coating. Composites: Mechanics, Computations, Applications, 7(2), 135–159.
3. Libove C, Hubka RE. Elastic Constants for Corrugated Core Sandwich Plates, NACA TN2289, 1951.
4. Vinson JR, The Behavior of Sandwich Structures of Isotropic and Composite Materials, Springer Science+Business Media, 2006.
5. Valdevit L, Wei Z, Mercer C, Zok FW, Evans AG. Structural performance of near-optimal sandwich panels with corrugated cores. International Journal of Solids and Structure 2006; 43(16):4888-4905.
6. Bartolozzi, G., Baldanzini, N., Pierini, M., & Zonfrillo, G. (2015). Static and dynamic experimental validation of analytical homogenization models for corrugated core sandwich panels. Composite Structures, 125, 343-353.
7. Boorle, R. K., & Mallick, P. K. (2016). Global bending response of composite sandwich plates with corrugated core: Part I: Effect of geometric parameters. Composite Structures, 141, 375-388.
8. Bitzer, T. N. Honeycomb technology: materials, design, manufacturing, applications and testing. Springer Science & Business Media, 2012.
9. Njuguna J. (ed.). Lightweight composite structures in transport: design, manufacturing, analysis and performance. – Woodhead publishing, 2016.
10. Vasiliev, V., & Morozov, E. V. (2013). Advanced mechanics of composite materials and structural elements. Newnes.
11. Bapanapalli SK, Martinez OM, Gogu C, Sankar BV, Haftka RT. Analysis and Design of Corrugated Core Sandwich Panels for Thermal Protection Systems of Space Vehicles. AIAA Paper 2006; 1942:1-18.
12. Martinez OA, Sankar BV, Haftka R, Bapanapalli SK, Blosser ML, Micromechanical Analysis of Composite Corrugated-Core Sandwich Panels for Integral Thermal Protection Systems. AIAA Journal 2007: 45(9):2323–2336.
13. Sharma A, Sankar BV, Haftka RT, Ebaugh NC. Multi-Fidelity Analysis of Corrugated-Core Sandwich Panels for Integrated Thermal Protection Systems. AIAA Journal 2009; 2009-2201:1–24.
14. Wei, K., Peng, Y., Qu, Z., He, R., & Cheng, X. (2017). High temperature mechanical behaviors of lightweight ceramic corrugated core sandwich panel. Composite Structures. Volume 176, 15 September 2017, Pages 379-387.
15. Lu, T. J., Valdevit, L., & Evans, A. G. (2005). Active cooling by metallic sandwich structures with periodic cores. Progress in Materials Science, 50(7), 789–815. http://doi.org/10.1016/j.pmatsci.2005.03.001
16. Gao, L., Sun, S., Zhao, Y., & Sun, Y. (2016). Thermostructural multiobjective optimization of a composite sandwich panel with lattice truss cores. Numerical Heat Transfer, Part B: *Fundamentals*, *70*(3), 233–250. http://doi.org/10.1080/10407790.2016.1193401
17. Xie G, Wang C, Ji T, Sunden B. Investigation on thermal and thermomechanical performances of actively cooled corrugated sandwich structures. Applied Thermal Engineering 2016; 103:660–669.
18. Leontiev, A. I. (1999). Heat and mass transfer problems for film cooling. Journal of Heat Transfer, 121(3), 509-527.
19. B. E. Gatewood, Thermal stresses, McGraw-Hill, New York, 1957, 232 p.
20. Timoshenko S, Gere J. Elastic Stability, 2nd Edition. McGraw-Hill Book Co., Inc., 1961.
21. Valdevit, L., Hutchinson, J. W., & Evans, A. G. (2004). Structurally optimized sandwich panels with prismatic cores. *International Journal of Solids and Structures*, *41*(18–19), 5105–5124. http://doi.org/10.1016/j.ijsolstr.2004.04.027
22. Heinz W. Bargmann (1985): Thermal buckling of elastic plates, Journal of Thermal Stresses, 8:1, 71-98
23. Formalev, V. F., Kolesnik, S. A., Chipashvili, A. A. (2006). An analytical investigation

of heat and mass transfer under conditions of film cooling of bodies. High temperature, 44(1), 108-114.

24. Karen, I., Yazici, M. and Shukla, A., 2016. Designing foam filled sandwich panels for blast mitigation using a hybrid evolutionary optimization algorithm. Composite Structures, 158, pp.72-82.
25. Han, B., Qin, K.K., Zhang, Q.C., Zhang, Q., Lu, T.J. and Lu, B.H., 2017. Free vibration and buckling of foam-filled composite corrugated sandwich plates under thermal loading. Composite Structures, 172, pp.173-189.